

Article

Water Electrolysis Anode Based on 430 Stainless Steel Coated with Cobalt Recycled from Li-Ion Batteries

Eric M. Garcia * and Hosane A. Taroco

Department of Exact and Biological Sciences, University of São João Del Rei—Sete Lagoas Campus, Sete Lagoas 35701-970, Brazil; hataroco@hotmail.com

* Correspondence: ericmgmg@hotmail.com; Tel./Fax: +55-31-3697-2003

Received: 4 August 2018; Accepted: 4 September 2018; Published: 6 September 2018

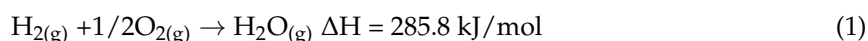


Abstract: In this paper, a new environmentally-friendly anode for hydrogen production was developed based on 430 stainless steel with an electrodeposited cobalt layer. The novelty of this work is the cobalt source once the electrodeposition bath was obtained from acid dissolution of a spent Li-ion battery cathode. The oxygen evolution reaction on electrodeposited cobalt in 1 M KOH is compatible with the E. Kobussen mechanism. The water discharge is related with reaction determinant step in low overpotential. The cobalt electrodeposition (3 Ccm^{-2}) promotes a significant improvement of 430 stainless steel anodic properties for oxygen evolution reaction. When the overpotential reaches 370 mV, the density current for 430 stainless steel with electrodeposit cobalt is $19 \text{ mA}\cdot\text{cm}^{-2}$ against $0.80 \text{ mA}\cdot\text{cm}^{-2}$ for 430 stainless steel without cobalt. Thus, the anode construction described in this paper is an excellent option for Li-ion battery recycling.

Keywords: Li-ion batteries; anode; cobalt recycling

1. Introduction

Renewable energy source such as hydrogen is considered crucial for a more sustainable future [1]. In fact, since daily processes even space exploration will depend, largely of hydrogen production within few years [2]. The hydrogen is considered environmentally friendly once the reaction between H_2 with O_2 molecules (forward direction in Equation (1)) has only water molecules as a sub-product, beyond high molar enthalpy value ($\Delta H = 285.8 \text{ kJ/mol}$ at 1013 mbar and 298 K) [2]. In this context, the water electrolysis is the most attractive route among the existed processes for very pure hydrogen production (and also O_2) in large scale (inverse direction in Equation (1)) [1].



In water electrolysis, the overpotential for oxygen evolution reaction (OER) is a limiting factor and responsible for the greatest energy loss source when the electrolysis is performed in alkaline or acid media [3,4]. However, alkaline media is preferred because in this condition the catalysts used in water electrolysis are more active and stable [4]. The OER also is present in others strategic power sources such as aqueous lithium air batteries [5], NiMH [3], and Zn-air [6]. Many papers are dedicated to investigate the alternative anode for OER with high efficiency [7]. The RuO_2 and IrO_2 are suggested as the benchmark for OER in alkaline solution [8]. However, these oxides have a prohibitive cost for large scale application [8]. Commercial electrodes for water electrolysis at an industrial scale must have important characteristics such as: high conductivity, high corrosion resistance, high catalytic effect for oxygen evolution reaction, and moreover low cost [9]. For Ni foam, the current density for OER is $10 \text{ mA}\cdot\text{cm}^{-2}$ in $\eta = 390 \text{ mV}$ (vs. NHE) in 0.5 M KOH. When the Ni foam receives a Co layer by electroless deposition ($\sim 2.3 \mu\text{m}$) the overpotential reduces for 270 mV [10]. This shows that a

cobalt layer around 2.3 μm is enough to decrease the overvoltage for OER approximately in 100 mV. Although the Ni anode has a good anodic behavior in OER, its cost is still high compared to the other substrates such as stainless steels. The Ni price is 8.66 US\$/Kg against 1.64 US\$/Kg and 0.450 US\$/Kg for 316SS and 430SS, respectively [11]. In this context, a special interest is devoted to stainless steel as anode for OER in alkaline solutions [9]. The literature reveals that the 316 stainless steel (316SS) shows a density current of $10 \text{ mA}\cdot\text{cm}^{-2}$ in $\eta = 370 \text{ mV}$ in $1.0 \text{ mol}\cdot\text{L}^{-1}$ KOH [12]. This value is similar to that found for Ni Foam in the same conditions [12]. This is expected since the 316 has 12% of Ni in its composition [13]. The 430SS has little more than 0.75% of Ni in its composition and approximately the same percentage of others alloys elements [13]. The low Ni content makes the 430SS cheaper, however, it is also less active for OER. [13]. Nevertheless, is possible improve the 430SS anodic properties with cobalt electrodeposition. The great advantage of this method is the possibility of cobalt recovery from Li-ion battery recycling [14].

Many papers describe the cobalt recycling from spent Li-ion batteries as a valuable and environmentally-friendly method [14–16]. Moreover, very pure cobalt can be obtained by acidic dissolution of lithium cobalt oxide (LiCoO_2) present in spent Li-ion battery cathode [16]. The recycling of LiCoO_2 is important, both economically and environmentally [16]. In this paper, we studied the application of 430SS, coated with recycled cobalt, as anode for OER in 1 M KOH solution. The cobalt used was obtained through dissolution of spent cathode of cell phones Li-ion batteries. The electrochemical characterization of this anode was accomplished through cyclic and linear voltammetry and electrochemical impedance spectroscopy (EIS).

2. Material and Methods

2.1. Preparation of Cobalt Electrodeposition Bath

The Li-ion battery used in this paper was chosen based on the LiCoO_2 presence as cathodic material [16]. The Li-battery used was of SAMSUNG[®] model SM-G530 (SANSUNG[®], China). The Li-ion battery was manually dismantled and physically separated into their different parts: anode, cathode, steel, separators, and current collectors. The cathode powder was washed with distilled water under agitation to facilitate the detachment of the active material from current collector. The Li-ion battery electrolyte is a nonaqueous solution composed of lithium salts, such as 1 M LiPF_6 , in alkyl organic carbonates (ethylene, propylene, and dimethyl carbonates) [17]. Thus, the spent cathode was heated at $200 \text{ }^\circ\text{C}$ for 5 h for eliminate the organic carbonates [17]. The active material was filtered and washed with distilled water to remove possible lithium salts such as LiPF_6 and LiClO_4 . The temperature of $40 \text{ }^\circ\text{C}$ degrees was maintained through a thermostatic bath. The recycled powder was dried in air for 24 h. A mass of 250.10 g of positive electrodes was dissolved in an aqueous solution containing 470.00 mL of $3.00 \text{ mol}\cdot\text{L}^{-1}$ H_2SO_4 and 30.00 mL of 30% (v/v) H_2O_2 . The LiCoO_2 acidic dissolution efficiency increases with acid concentration [17–19]. The H_2O_2 reduces the Co^{3+} , insoluble in water, to the Co^{2+} , soluble in aqueous solution. This behavior is represented by the chemical equation of the dissolution process (Equation (2)) [18].



In order to obtain the cobalt electrodeposition bath, the system was maintained under constant magnetic agitation at $80 \text{ }^\circ\text{C}$ for 2 h. The filtration was performed for separation of carbonaceous material and for obtention of cobalt electrodeposition bath.

The concentrations of Mn, Ni, and Cu were analyzed with atomic absorption spectrophotometry (AAS) on a Hitachi-Z 8200 and the values were below of detection limit ($10^{-5} \text{ mol}\cdot\text{L}^{-1}$). The concentration of Co^{2+} was adjusted for $1 \text{ mol}\cdot\text{L}^{-1}$ and the solid NaOH was used for adjust the $\text{pH} = 3$ [20]. The pH of electrodeposition bath was maintained equal to 3.0 and the cobalt concentration was $1.00 \text{ mol}\cdot\text{L}^{-1}$. This high concentration was chosen to increase the electrodeposition efficiency [16–20].

2.2. Electrochemical Measurements

Electrochemical measurements were made using an IVIUM power supply (Ivium Technologies BV, De Zaale, The Netherlands). The working electrode was made of commercial ferritic stainless steel 430 (430SS). The steel samples were prepared as rectangular foils with a geometric area of 1.00 cm². The auxiliary electrode, with an area of 3.75 cm², was made of platinum. A saturated calomel electrode (SCE) reference electrode was used. The AC-impedance measurements were carried out over the frequency range of 10⁴ to 10⁻² Hz at the rest potentials. The Nyquist diagrams were adjusted with the IVIUMSOFT. The conversion for reversible hydrogen electrode (RHE) was made using the Equation (3) and the overpotential (η) was calculated using Equation (4) [9].

$$E_{(\text{RHE})} = E_{(\text{SCE})} + (0.059\text{pH} + 0.042) \quad (3)$$

$$\eta = E_{(\text{SCE})} + (0.059\text{pH} + 0.042) - 1.23\text{V} \quad (4)$$

The working electrodes were sanded with 600-grit sandpaper before each measurement and washed with distilled water. All the electrochemical measurements were performed without solution agitation, at 25 °C. The bath used in cobalt electrodeposition was obtained by acidic dissolution of spent cathode of Li-ion batteries. The potential used for electrodeposition of cobalt onto 430SS was -1.0 V. The charge density was controlled in 3 Ccm⁻² [9]. The scanning electron microscope JEOL JXAmodel 8900 RL (JEOL, Peabody, MA, USA) was used for surface morphology observations. The cobalt electrodeposit was characterized by X-ray diffraction on a 200 B Rotaflex-Rigaku (Rigaku, Tokyo, Japan) with Cu K α irradiation, a Cu filter, and scanning speed of 2°·min⁻¹.

3. Results and Discussion

3.1. Characterization of Electrodeposited Cobalt onto 430SS

Figure 1 shows the cyclic voltammetry obtained by electrodeposition of cobalt on 430SS. The starting potential was -0.5 V (rest potential). Sweeping in the direct direction is observed an increase of the cathodic current from -1 V. Some studies of cobalt electrodeposition in pH ≥ 4 , proposes that the mechanism involves the formation of Co(OH)₂ and the subsequent reduction of cobalt hydroxide to metallic cobalt [17–20]. Considering the pH used in this study (pH = 3), the presence of other phases, such as Co(OH)₂, in the cobalt electrodeposit was not expected [20].

Figure 2 shows the scanning electron microscopy (SEM) of electrodeposited cobalt. The morphology of electrodeposited cobalt is commonly observed in other papers [15,16].

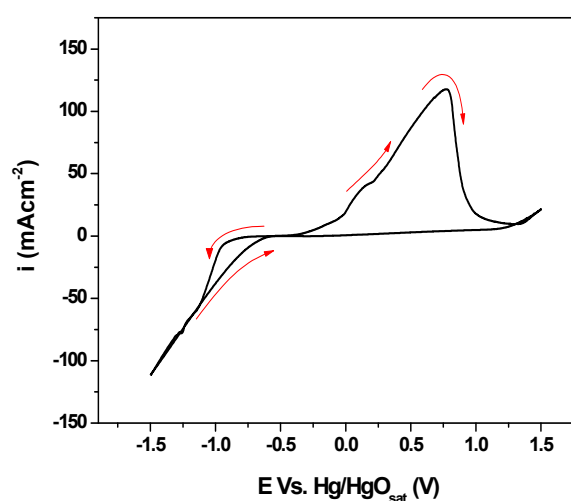


Figure 1. Cyclic voltammetry of 430SS in a with (black line) and without (red line) electrodeposited cobalt (scan rate 10 mV·s⁻¹).

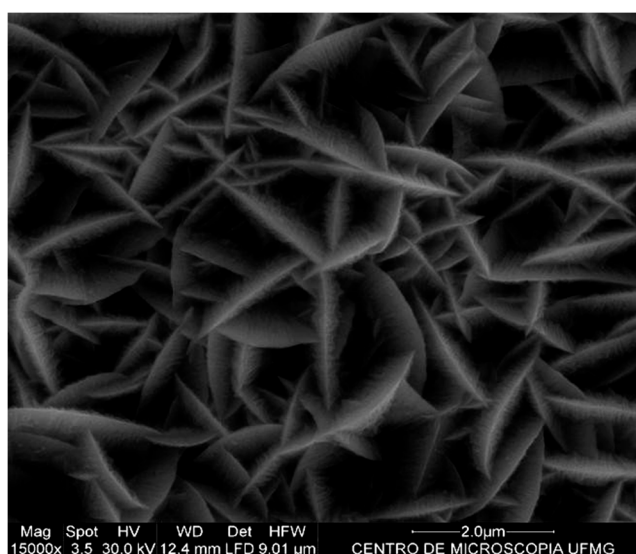


Figure 2. SEM of electrodeposited cobalt onto 430SS with magnification 15,000 \times .

The Figure 3 shows the X-ray diffraction of 430SS with (black line) and without (red line) electrodeposited cobalt. The XDR was compared with the JCPDS card for cobalt in hexagonal compact phase (hcp) (no. 05-0727) and face centered cubic phase (fcc) (no. 15-0806). The presence of both hcp and fcc phases in electrodeposited cobalt also described in the literature [16–20]. No peaks related to the $\text{Co}(\text{OH})_2$ phase were observed, which may be an indication that the cobalt electrodeposition mechanism does not involves this intermediate [20].

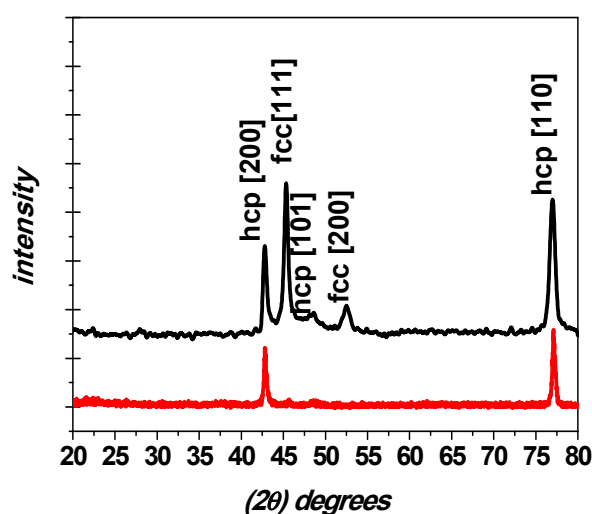


Figure 3. X-ray diffraction (DRX) of 430SS with (black line) and without (red line) electrodeposited cobalt.

Figure 4 shows the cyclic voltammetry of 430SS with cobalt coating (430SS/Co) in $1.0 \text{ mol}\cdot\text{L}^{-1}$ KOH. The first peak (A_1) is due the formation of $\text{Co}(\text{OH})_2$ layer onto cobalt previously electrodeposited [14,21]. The peak A_2 is related to oxidation of Co^{2+} to Co^{3+} due formation of monometallic layered double hydroxides (LDH) onto electrodeposited cobalt [21]. The A_2 can also be related with Co_3O_4 formation [22,23]. The peak A_3 is relative to electrochemical reaction related to conversion of Co^{3+} to Co^{4+} [14]. The formation of Co^{4+} is important because in alkaline media the OER generally involves the OH^- adsorption as first step (Equation (5)). Thus, a transition metal ion with multiple valences and strong bonding power is

necessary [21]. Equation (5) represents the adsorption of OH⁻ by charged transition metal (Mⁿ⁺) in the hydroxide/oxide crystalline net.

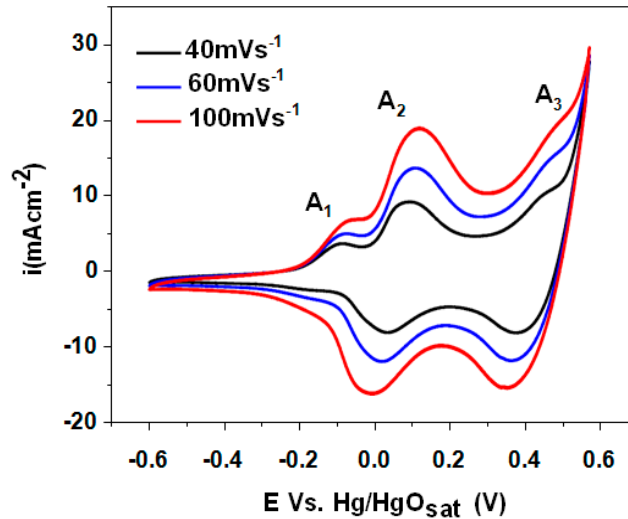
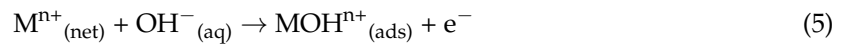


Figure 4. Cyclic voltammetry of 430SS and 430SS/Co in 1 mol·L⁻¹ KOH with different scan rates.

3.2. Mechanism of Oxygen Evolution

Before study the electrochemical behavior of 430SS coated with recycled cobalt as an anode in water electrolysis, some theoretical considerations need to be performed [24,25]. The most commonly proposed OER pathway for Co oxides is due to the E. Kobussen mechanism [24]. For this mechanism, only the first two steps have significant importance [24,25]. Initially, the hydroxyl ions are absorbed in the active sites, where ‘S’ is the non-occupied active sites (Equation (6)). The reaction determining step (rds) is the water discharge, where ‘SOH’ is the occupied active sites (Equation (7)). If water discharge (Equation (7)) is the rds, the first step (Equation (6)) is in quasi-equilibrium conditions. The anodic and cathodic current are approximately equals, thus the Nerstian equilibrium can be considered in terms of occupied (SOH = θ) and non-occupied (S = 1 – θ) sites. The total current (i₁) for first step can be represented by Equation (8) where:

F: The Faraday constant.

η: the overpotential.

k₁ and k₋₁: The direct and inverse velocity constant rate, respectively, for the first step.

R: The ideal gas constant (8.314 J·mol⁻¹).

T: The absolute temperature (K).

α: The symmetry coefficient of charge transfer barrier.



$$i_1 = Fk_1\theta[OH^{-}]e^{\left[\frac{(1-\alpha)F\eta}{RT}\right]} - Fk_{-1}(1-\theta)e^{-\left[\frac{\alpha F\eta}{RT}\right]} \tag{8}$$

Since the current represented by the Equation (8) is approximately zero, one can obtain the relation of non-occupied and occupied sites on the electrode surface (Equation (9)).

$$\frac{\theta}{(1-\theta)} = \frac{k_1}{k_{-1}} [\text{OH}^-] e^{\frac{F\eta}{RT}} \quad (9)$$

When the ΔH of adsorption varies with surface covered, the Temkin isotherm more appropriately describes the electrochemical interface. To represent coverage-dependent deviations in adsorption free energy from Langmuir conditions (Equation (9)), the covering dependent function $r\theta$ is added where r is a coefficient of increase in adsorption energy (Equation (10)) [24,25].

$$\frac{\theta}{(1-\theta)} = K_2 [\text{OH}^-] e^{\frac{F\eta}{RT}} e^{\frac{-\Delta G^0 + r}{RT}} \quad (10)$$

If one considers a region in which $0.2 < \theta < 0.8$ the variation of $\ln\left(\frac{\theta}{1-\theta}\right)$ is much less than that of the term $e^{r\theta/RT}$, thus the term in parenthesis in the Equation (10) is practically constant. The function $r\theta$ can be given as a function of the overpotential and the concentration of hydroxyl ions (Equations (11) and (12)).

$$r\theta = \left[\ln\left(\frac{\theta}{(1-\theta)}\right) RT + RT \ln - \Delta G^0 + RT \ln [\text{OH}^-] \right] + F\eta \quad (11)$$

$$r\theta = K_3 + F\eta \quad (12)$$

$$K_3 = \left[\ln\left(\frac{\theta}{(1-\theta)}\right) RT + RT \ln - \Delta G^0 + RT \ln [\text{OH}^-] \right]$$

The equation for the rate determining step (rds) can be written as shown in the Equation (13) where δ is a symmetry factor ($0 < \delta < 1$) for the adsorption process, which depends in magnitude and form of the activation energy barrier. Replacing Equation (12) in Equation (13), the Tafel coefficient is obtained for rds considering a possible situation where $\alpha = 0.5$ and $\delta = 0.5$ (Equation (14)).

$$i_2 F k_2 \theta [\text{OH}^-] e^{\frac{(1-\alpha)F\eta}{RT}} e^{\frac{(1-\delta)E}{RT}} \quad (13)$$

$$\left(\frac{d \ln i_2}{d \eta} \right) = \frac{F\eta}{RT} \quad (14)$$

Figure 5 compares the linear voltammetry of 430SS and 430SS/Co in a $1.0 \text{ mol}\cdot\text{L}^{-1}$ KOH. The cobalt electrodeposition significantly reduces the onset potential for oxygen evolution reaction (OER). The onset potential for OER onto 430SS occurs around $\eta = 380 \text{ mV}$. By other hand, for 430SS/co the onset potential is around $\eta = 280 \text{ mV}$. The onset potential was compatible with that obtained in the literature for metallic cobalt [25]. The Tafel coefficient $\left(\frac{d \ln i}{d \eta}\right)$ was calculated for both electrode and for 430SS. Only one distinct region was found with $\frac{d \ln i}{d \eta} = 38.94 \text{ V}^{-1}$ ($\sim 59 \text{ mV}\cdot\text{dec}^{-1}$). Considering $T = 298 \text{ K}$, this Tafel coefficient agree with rds related with water discharge (Equation (14)). For 430SS/Co, two distinct regions are found in linear voltammetry. The first region agrees with water discharge as rds ($59 \text{ mV}\cdot\text{dec}^{-1}$). The second region has a Tafel coefficient around $118 \text{ mV}\cdot\text{dec}^{-1}$. In this region there is a high degree of coverage of adsorbed species [25]. Thus, the rds for the OER is mainly due to the step described by Equation (6). One can observe that the cobalt electrodeposition (3 Ccm^{-2}) promotes a significant improvement of 430SS anodic properties for OER. When the overpotential reaches 370 mV , the density current for 430SS/Co is $19 \text{ mA}\cdot\text{cm}^{-2}$ against $0.80 \text{ mA}\cdot\text{cm}^{-2}$ for 430SS. The 430SS/Co exhibits the double of density current to OER if compared with 316SS [9] or Ni foam [12]. Considering the linear voltammetry of metallic cobalt in 1 M KOH , the literature describes a value around $10 \text{ mA}\cdot\text{cm}^{-2}$ of density current of OER when the overpotential is around 370 mV [25]. Probably due to a surface area effect, the density current found in this work is approximately double. This shows the advantage of working with cobalt electrodeposition.

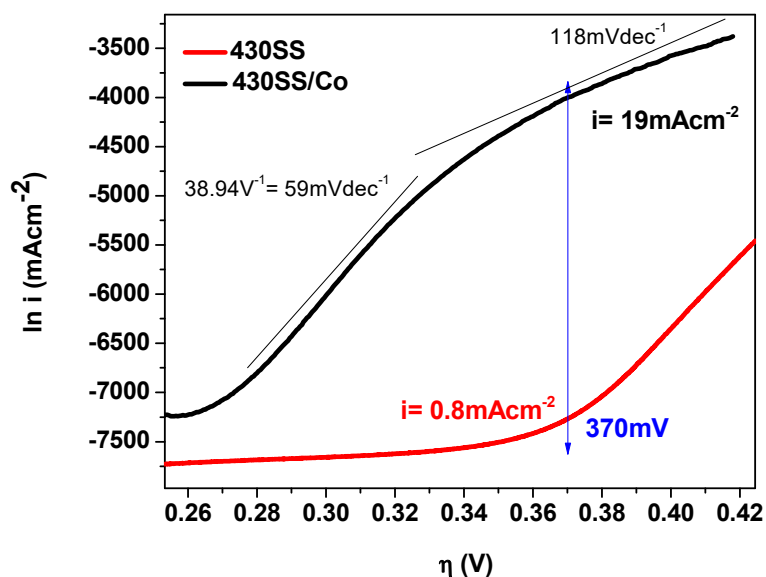


Figure 5. Linear voltammery of 430SS and 430SS/Co in $1 \text{ mol}\cdot\text{L}^{-1}$ KOH with scan rate equal to $1 \text{ mV}\cdot\text{s}^{-1}$.

3.3. Electrochemical Performance

The electrochemical interfacial process is better investigated using electrochemical impedance spectroscopy (EIS). Figures 6 and 7 compares the EIS measures of 430 stainless steel (430SS) and 430 stainless steel with recycled metallic cobalt coating (430SS/Co) in a $1.0 \text{ mol}\cdot\text{L}^{-1}$ KOH after cyclic voltammery study. The R_1 is related with the resistance of ionic motion in the solution bulk, R_2 and R_3 are the polarization resistances and C_{dl} is a non-ideal capacitance of double layer. For EIS of 430SS (Figure 6) the interface is compatible with Randles circuit [24]. However, for 430SS/Co (Figure 7) the LDH formed onto electrodeposited cobalt behaves as a supercapacitor, thus two constant-phase elements must be taken into account as shown in Figure 7 [21].

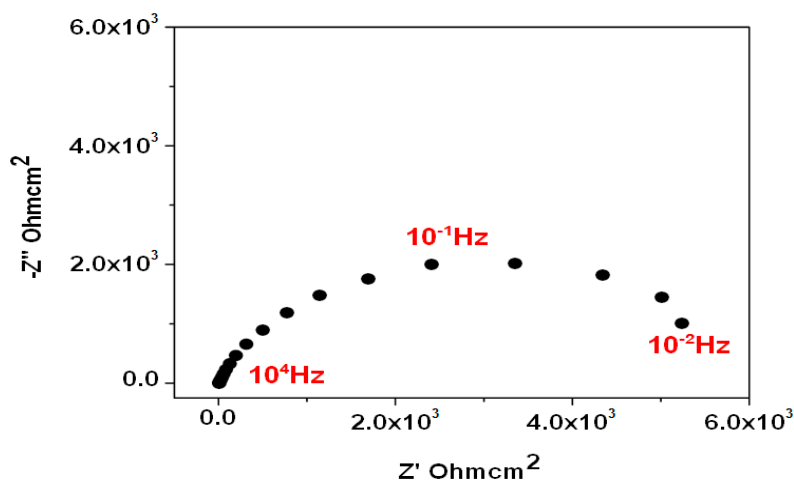


Figure 6. Cont.

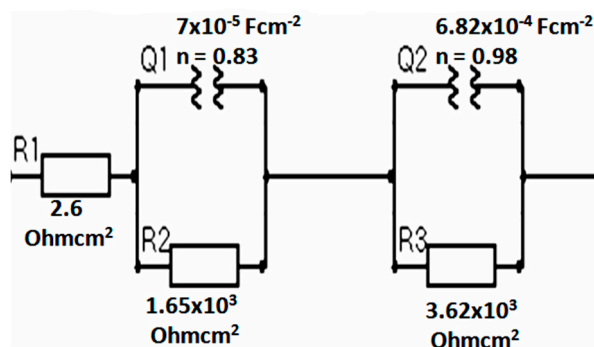


Figure 6. Electrochemical impedance spectroscopy for 430SS in 1 M KOH and the adjusted electrical circuit.

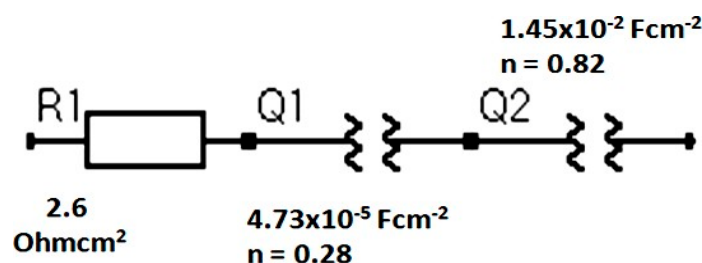
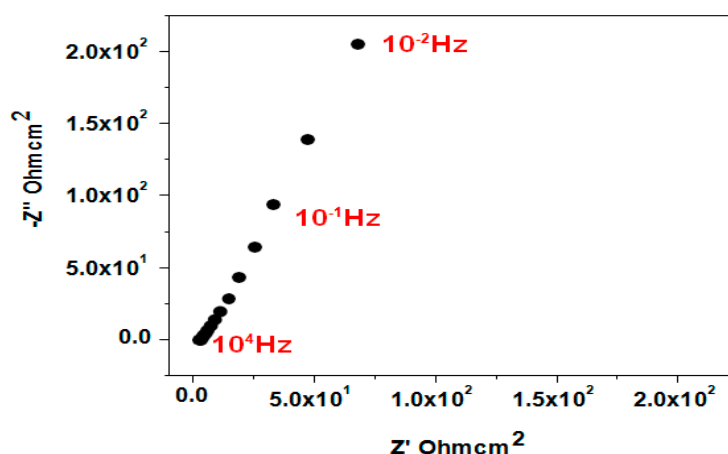


Figure 7. Electrochemical impedance spectroscopy for 430SS/Co in 1 M KOH and the adjusted electrical circuit.

4. Conclusions

In this paper, a new anode for hydrogen production was developed based on 430 stainless steel with an electrodeposited cobalt layer. The novelty of this work is the cobalt source once the electrodeposition bath is obtained of acid dissolution of Li-ion batteries spent cathode. The electrodeposited cobalt in 1 M KOH behaves as supercapacitor. Considering the linear voltammetry in 1 M KOH, when the overpotential reaches 370 mV, the anodic density current for 430SS/Co is $19 \text{ mA}\cdot\text{cm}^{-2}$ against $0.80 \text{ mA}\cdot\text{cm}^{-2}$ for 430SS. Thus, the anode construction described in this paper is an excellent option for Li-ion battery recycling. Future work must be performed to study the reproducibility of the OER catalytic performance once the materials collected from spent batteries vary in composition.

Author Contributions: H.A.T. and E.M.G. analyzed the data and prepared the manuscript.

Funding: This work was supported by CNPq, Federal University of São João Del Rei UFSJ/Sete Lagoas/DECEB, UFSJ/DCNAT, Programa de Pós-Graduação Multicêntrico em Química (PPGMQ), and Rede Mineira de Química.

Conflicts of Interest: The authors declare no conflict of interest.

References

1. Kjartansdóttir, C.K.; Nielsen, L.P.; Møller, P. Development of durable and efficient electrodes for large-scale alkaline water electrolysis. *Int. J. Hydrogen Energy* **2013**, *38*, 8221–8231. [CrossRef]
2. Belz, S. A synergetic use of hydrogen and fuel cells in human spaceflight power systems. *Acta Astronaut.* **2016**, *121*, 323–331. [CrossRef]
3. Guo, D.; Shangguan, E.; Li, J.; Zhao, T.; Chang, Z.; Li, Q.; Yuan, X.Z.; Wang, H. Effects of γ -CoOOH coating on the high-temperature and high-rate performances of spherical nickel hydroxide electrodes. *Int. J. Hydrogen Energy* **2014**, *39*, 3895–3903. [CrossRef]
4. Marinia, S.; Salvi, P.; Nellia, P.; Pesenti, R.; Villa, M.; Berrettoni, M.; Zangari, G.; Kiros, Y. Advanced alkaline water electrolysis. *Electrochim. Acta* **2012**, *82*, 384–391. [CrossRef]
5. Moureaux, F.; Stevens, P.; Toussaint, G.; Chatenet, M. Development of an oxygen-evolution electrode from 316L stainless steel: Application to the oxygen evolution reaction in aqueous lithium-air batteries. *J. Power Sources* **2013**, *229*, 123–132. [CrossRef]
6. Li, P.C.; Chien, Y.J.; Hu, C.C. Novel configuration of bifunctional air electrodes for rechargeable zinc-air batteries. *J. Power Sources* **2016**, *313*, 37–45. [CrossRef]
7. Wang, H.; Li, Z.; Li, G.; Peng, F.; Yu, H. $\text{Co}_3\text{S}_4/\text{NCNTs}$: A catalyst for oxygen evolution reaction. *Catal. Today* **2015**, *245*, 74–78. [CrossRef]
8. Giordano, L.; Han, B.; Risch, M.; Hong, W.T.; Rao, R.R.; Stoerzinger, K.A.; Horn, Y.S. pH dependence of OER activity of oxides: Current and future perspectives. *Catal. Today* **2016**, *262*, 2–10. [CrossRef]
9. Yu, F.; Li, F.; Sun, L. Stainless steel as an efficient electrocatalyst for water oxidation in alkaline solution. *Int. J. Hydrogen Energy* **2016**, *41*, 5230–5233. [CrossRef]
10. Alonso, F.J.P.; Adán, C.; Rojas, S.; Peña, M.A.; Fierro, J.L.G. Ni-Co electrodes prepared by electroless-plating deposition. A study of their electrocatalytic activity for the hydrogen and oxygen evolution reactions. *Int. J. Hydrogen Energy* **2015**, *40*, 51–61. [CrossRef]
11. ARGUS Metal Prices. Available online: <https://www.argusmedia.com/metals/argus-metal-prices> (accessed on 12 May 2018).
12. Liang, Y.; Liu, Q.; Asiri, A.M.; Sun, X.; He, Y. Nickel-Iron foam as a three-dimensional robust oxygen evolution electrode with high activity. *Int. J. Hydrogen Energy* **2015**, *40*, 13258–13263. [CrossRef]
13. Ramírez, J.M.O.; Cornelio, M.L.C.; Godínez, J.U.; Arco, E.B.; Castellanos, R.H. Studies on the hydrogen evolution reaction on different stainless steels. *Int. J. Hydrogen Energy* **2007**, *32*, 3170–3173. [CrossRef]
14. Gonçalves, S.A.; Garcia, E.M.; Taroco, H.A.; Teixeira, R.G.; Guedes, K.J.; Gorgulho, H.F.; Martelli, P.B.; Fernandes, A.P.L. Development of non-enzymatic glucose sensor using recycled cobalt from cell phone Li-ion batteries. *Waste Manag.* **2015**, *46*, 497–502. [CrossRef] [PubMed]
15. Garcia, E.M.; Taroco, H.A.; Matencio, T.; Domingues, R.Z.; Santos, J.A.F.; Freitas, M.B.J.G. Electrochemical recycling of cobalt from spent cathodes of lithium-ion batteries: Its application as coating on SOFC interconnects. *J. Appl. Electrochem.* **2011**, *41*, 1373–1379. [CrossRef]
16. Freitas, M.B.J.G.; Garcia, E.M. Electrochemical recycling of cobalt from cathodes of spent lithium-ion batteries. *J. Power Sources* **2007**, *171*, 953–959. [CrossRef]
17. Garcia, E.M.; Taroco, H.A.; Madeira, A.P.C.; Souza, A.G.; Silva, R.R.; Melo, J.O.; Taroco, C.G.; Teixeira, Q.C. Application of Spent Li-Ion Batteries Cathode in Methylene Blue Dye Discoloration. *J. Chem.* **2017**, *2017*, 3621084. [CrossRef]
18. Garcia, E.M.; Vanessa de Freitas, C.L.; Tarôco, H.A.; Matencio, T.; Domingues, R.Z.; dos Santos, J.A. The anode environmentally friendly for water electrolysis based in LiCoO_2 recycled from spent lithium-ion batteries. *Int. J. Hydrogen Energy* **2012**, *37*, 16795–16799. [CrossRef]
19. Garcia, E.; Taroco, H.; Teixeira, R. Fast Electrochemical Method for Organic Dye Decolorization Using Recycled Li-Ion Batteries. *Recycling* **2018**, *3*, 35. [CrossRef]
20. Garcia, E.M.; Taroco, H.A.; Domingues, R.Z.; Matencio, T.; Gonçalves, S.L. Electrochemical recycling of cell phone Li-ion batteries: Application as corrosion protector of AISI 430 stainless steel in artificial seawater. *Ionics* **2016**, *22*, 735–740. [CrossRef]
21. Vialat, P.; Rabu, P.; Mousty, C.; Leroux, F. Insight of an easy topochemical oxidative reaction in obtaining high performance electrochemical capacitor based on CoII CoIII monometallic cobalt layered double hydroxide. *J. Power Sources* **2015**, *293*, 1–10. [CrossRef]

22. Ko, J.M.; Soundarajan, D.; Park, J.H.; Yang, S.D.; Kim, S.W.; Kim, K.M.; Yu, K.H. γ -Ray-induced synthesis and electrochemical properties of a mesoporous layer-structured α -Co(OH)₂ for supercapacitor applications. *Curr. Appl. Phys.* **2012**, *12*, 341–345. [[CrossRef](#)]
23. Panga, M.; Long, G.; Jiang, S.; Ji, Y.; Han, W.; Wang, B.; Liu, X.; Xi, Y.; Wang, D.; Xu, F. Ethanol-assisted solvothermal synthesis of porous nanostructured cobalt oxides (CoO/Co₃O₄) for high-performance supercapacitors. *Chem. Eng. J.* **2015**, *280*, 377–384. [[CrossRef](#)]
24. Garcia, E.M.; Tarôco, H.A.; Matencio, T.; Domingues, R.Z.; dos Santos, J.A. Electrochemical study of La_{0.6}Sr_{0.4}Co_{0.8}Fe_{0.2}O₃ during oxygen evolution reaction. *Int. J. Hydrogen Energy* **2012**, *37*, 6400–6406. [[CrossRef](#)]
25. Lyons, M.E.; Brandon, M.P. The oxygen evolution reaction on passive oxide covered transition metal electrodes in alkaline solution part II—Cobalt. *Int. J. Electrochem. Sci.* **2008**, *3*, 1425–1462.



© 2018 by the authors. Licensee MDPI, Basel, Switzerland. This article is an open access article distributed under the terms and conditions of the Creative Commons Attribution (CC BY) license (<http://creativecommons.org/licenses/by/4.0/>).